THE JOURNAL OF PHYSICAL CHEMISTRY B

Article

pubs.acs.org/JPCB

Macroscopic and Microscopic Study of 1-Ethyl-3-methyl-imidazolium Acetate−Water Mixtures

Craig A. Hall,[†] Kim A. Le,[‡] Cyrielle Rudaz,[‡] Asanah Radhi,[†] Christopher S. Lovell,[†] Robin A. Damion,[†] Tatiana Budtova,[‡] and Michael E. Ries*[,†]

[†]School of Physics and Astronomy, University of Leeds, Leeds LS2 9JT, United Kingdom

[‡]Centre de Mise en Forme des Matériaux, MINES ParisTech, UMR CNRS 7635, rue Claude Daunesse, BP 207, 06904 Sophia Antipolis, France

ABSTRACT: Mixtures of 1-ethyl-3-methyl-imidazolium acetate ([C2mim][OAc]) and water across the entire composition range, from pure [C2mim][OAc] to pure water, have been investigated using density, viscosity, and NMR spectroscopy, relaxometry, and diffusion measurements. These results have been compared to ideal mixing laws for the microscopic data obtained from the NMR results and macroscopic data through the viscosity and density. It was also found that the mixing of the two fluids is exothermal. The proton spectra indicate though that [C2mim][OAc] and water are interacting without the formation of new compounds. The maximal deviations of experimental data from theoretical mixing rules were all found to occur within the range 0.74 ± 0.06 mol fraction of water, corresponding to approximately three water molecules per [C2mim][OAc] molecule.

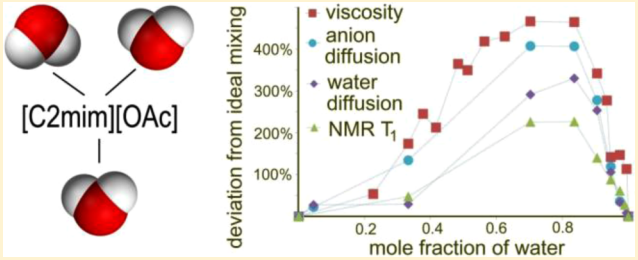

INTRODUCTION

The term ionic liquid (IL) has come to mean a salt that, due to its poorly coordinating ions, is in the liquid state below 100 °C.[1] For a long time ILs have been considered mostly as media for doing electrochemistry. Recently there has been a great deal of interest in ILs because of their ability to act as versatile solvents, especially for some difficult to dissolve polysaccharides such as cellulose.[2] This along with some of their other properties—negligible vapor pressure, high thermal stability, and nonflammability—have made them very desirable for use as "green" solvents in industry.

Most ILs are hygroscopic,[3] and even those that are so-called hydrophobic[4] have the ability to absorb water. From the point of view of industrial processes using ILs, it is important that the role of water mixed or absorbed is well understood, as avoiding contamination by water on a large scale could prove both difficult and costly. The presence of water in an IL can change many of the properties of the IL such as its conductivity, polarity, and viscosity and also key desirable properties such as the dissolution power toward the substance that is to be chemically modified or processed from the solution.

Molecular dynamics simulations[5−9] and experiments[10−13] have been used to probe the structures formed in ILs as water is added to them. Particular attention has been paid to imidazolium-based ILs where it is thought that water interacts strongly with the imidazolium ring of the cation.[1,7] For example, it is known that without water imidazolium cations, which are geometrically larger than their anions, surprisingly diffuse faster than their anion.[14] Interestingly, the addition of a small amount of water to these systems, for example 1-ethyl-3-methylimidazolium ethylsulfate and triflate, causes this "anomalous" diffusion to be reduced, with both the cation and anion tending to similar values for their self-diffusion coefficients.[3]

In this work we concentrate on the influence of water on the properties of the imidazolium-based IL, 1-ethyl-3-methyl-imidazolium acetate ([C2mim][OAc]). Our motivation is that this particular imidazolium based IL is a very promising solvent for cellulose, a polysaccharide that does not melt.[14,15] The only way to process cellulose is therefore to dissolve or derivatize it. There is an ongoing search for easy-to-handle and nontoxic solvents for this naturally occurring, highly abundant, organic macromolecule. The understanding of the solution properties is therefore necessary for the successful processing and performing of chemical modifications of the solute. Water is a cellulose nonsolvent and used for cellulose coagulation. Even a low amount of water, 15−20% by weight, can drastically change the state of cellulose, from dissolved to coagulated. The first steps in the understanding of the role of water in cellulose−[C2mim][OAc] solutions were published by Le et al.[16] It was reported there that heat was produced when mixing [C2mim][OAc] and water indicating that interactions are occurring between the components. However, the properties of the [C2mim][OAc]−water system remain to be quantified, and that is the purpose of this publication.

Received: July 10, 2012
Revised: September 22, 2012
Published: September 28, 2012

dx.doi.org/10.1021/jp306829c | J. Phys. Chem. B 2012, 116, 12810−12818

To the best of our knowledge there is only one experimental article on the properties of [C2mim][OAc]−water mixtures.[17] It describes a strong viscosity decrease with the addition of water (determined at 25 °C) as would be expected. The excess enthalpy when mixing various $[C2MIM]^+$ and 1-butyl-3-methylimidazolium containing salts with water has been reported,[1] and these results were interpreted as showing that there are "stronger" interactions between IL and water, compared with respective IL−IL and water−water interactions. Most of the literature agrees on the formation of aggregates or micelles of an IL in water, similar to ionic surfactant behavior.[18−23] Hydrogen bonding between some ILs and water has been observed experimentally (using NMR and IR) and confirmed with molecular modeling.[24,25] Structural organization of water around dissociated ions has also been reported based on IR, viscosity, conductivity, and refractive index measurements.[26,27]

In this study we investigate [C2mim][OAc]−water mixtures across the entire composition range, from pure [C2mim][OAc] to pure water and across a range of temperatures. [C2mim][OAc] is an IL that is fully miscible with water. The goal of this work is to understand and correlate [C2mim][OAc]−water macroscopic properties (viscosity and density) to microscopic properties (molecular translational and rotational dynamics). We employ rheology, high field NMR self-diffusion, and low field NMR relaxometry. This allows us to determine how much the parameters (viscosity and diffusion coefficient) deviate from simple ideal mixing rules.[28−30] Furthermore, by comparing the NMR data with the rheological measurements, via Stokes−Einstein type analyses, we determine how the local, molecular level viscosity is related to the macroscopic measured zero shear rate viscosity.

The work is structured as follows. First we make a brief overview of background approaches developed for mixtures, the so-called "ideal mixing rules", and suggest how it can be applied to the results we obtain from various experimental techniques. The presentation of experimental results starts with showing "simple" measurements (mixture temperature, density) which indicate that [C2mim][OAc] and water are interacting. Then we show viscosity, NMR relaxometry and diffusion experimental results and discuss the behavior of each parameter in the view of their "ideal mixing rule". Finally, we consider all parameters together and analyze their deviation from the ideal mixing rule as a function of the amount of water added to [C2mim][OAc].

EXPERIMENTAL METHODS

Materials. [C2mim][OAc] (>90% purity) was used as received from Sigma Aldrich for viscosity, density, and mixture temperature measurements. For the NMR measurements [C2mim][OAc] (97% purity) was used as received from Sigma Aldrich. Distilled water was used to form the [C2mim][OAc]−water mixtures. Mixtures were prepared in weight and mole fractions were subsequently calculated.

NMR Sample Preparation. Mixing was achieved by stirring [C2mim][OAc] and water in an MBraun Labmaster 130 Atmospheric Chamber under nitrogen. The chamber is maintained at a dewpoint level between −70 and −40 °C. We followed the recommendations set out by Annat et al.,[31] such as keeping sample depths to less than 1 cm to minimize convection currents on heating in the NMR spectrometer. The sample tubes were then permanently sealed to prevent contamination with water vapor from the air. Finally the tubes were shaken and then left to settle for 24 h to make sure the mixtures were homogeneous. From our NMR spectra and previous work, we estimate the uncertainty in water content to be <0.5% by weight.[14]

NMR Relaxometry. The spin−lattice relaxation time T_1 and spin−spin relaxation time T_2 were measured for each of our samples in steps of 10 °C between 20 and 90 °C inclusive using a 20 MHz Maran Benchtop NMR spectrometer. The inversion recovery method was used to determine T_1 and the Carr−Purcell−Meiboom−Gill[32,33] pulse sequence for T_2. At each temperature the samples were left to equilibrate for 10 min before measurements were taken.

NMR Diffusion. The self-diffusion coefficients of all of the species were determined by a pulsed-field gradient technique using a Bruker Avance II 400 MHz spectrometer with a diffusion probe (Diff60) capable of producing field gradients of up to 24 T m^{-1}. The measurements were taken using a stimulated echo pulse sequence with bipolar gradients.[31] The calibration of the gradient field strength was performed by measuring the self-diffusion coefficient of water at 20.0 ± 0.1 °C which has the value[34] (2.03 ± 0.01) × 10^{-9} m^2 s^{-1}. A subsequent calibration of the sample temperature was performed by measuring the temperature dependence of the diffusion coefficient of water with reference to results published by Holz et al.[34]

The attenuation of the signal intensity in this PFG NMR experiment is given by[35]

$$\ln(S_i/S_{i0}) = -D_i\gamma^2 g^2 \delta^2(\Delta - \delta/3 - \tau/2) \quad (1)$$

where S_i is the measured signal intensity of species i, D_i is the self-diffusion coefficient of that species, S_{i0} defines the initial signal intensity, γ is the proton gyromagnetic ratio, δ is the pulse duration of a combined pair of bipolar pulses, τ is the period between bipolar gradients, Δ is the period separating the beginning of each pulse-pair (i.e., diffusion time), and g is the gradient strength. In each individual experiment the strength of the gradient pulse was incremented while δ and Δ remained constant. τ was kept constant at 2 ms.

Viscosity. The viscosities of the various solutions were measured on stress-controlled Bohlin GeminiTM 150 rheometer (Malvern Instruments, U.K.) with a Peltier plate for temperature control. The measuring cell was of cone−plate geometry (4°−40 mm). The viscosity−-shear rate dependence was recorded at each temperature between 10 and 50 °C in steps of 5 °C. To prevent the uptake of water vapor from the air a thin film of low-viscosity silicone oil was placed at the edge of the gap. It is estimated that the uncertainty in viscosity values is less than 10%.

Density. Mixture density was measured with a standard pycnometer at 27 °C temperature. The error in density was estimated to be 2%.

Mixing Temperature. Temperature change due to the addition of water to [C2mim][OAc] was recorded using an electronic contact thermometer VT-5 with a PT1000 probe. The experiments were performed at room temperature, and starting components were also at room temperature. Ten ml of [C2mim][OAc] was the starting volume. A given amount of water, from 1 to 50 mL, was added to [C2mim][OAc], and the temperature evolution in time during the first 10−15 min was measured under gentle mixing. Attention will be paid to the temperature change of the mixture within the first 100 s; in the first approximation, thermal exchange with the surrounding medium will be thus neglected.

BACKGROUND: IDEAL MIXING LAWS

The viscosity of liquid mixtures has attracted much attention in the literature, from the simply practical perspective of being able to predict resultant viscosities to the more theoretical with the aim of gaining a deeper understanding of the interactions between the components.[29] In the seminal paper by Powell, Roseveare, and Eyring a general theory of viscosity, diffusion, and thermal and ionic conductivities in terms of a statistical mechanical theory of reaction rate was developed.[30] To model viscous flow a shearing force is applied across two layers of molecules, and flow takes place when a single molecule pushes past its neighbor and falls into a vacant equilibrium position, termed a hole. An activation energy is required for a molecule to jump over its neighbor and the effect of the shear force acting on the molecules is to help the forward and hinder the backward movement of the molecules, making the former more energetically favorable and the latter less so. The authors show that there is a close link between flow and vaporization, as the same bonds that need to be broken for flow to take place are necessary to be broken for vaporization. For associated liquids it is the breaking of hydrogen bonds that becomes the important factor.

The work by Powell et al. also included the case of liquid mixtures consisting of molecules with different sizes interdiffusing. In mixtures the ease of a molecule to flow is not determined primarily by its own properties but more by the readiness with which the "solvent" contributes holes for it to flow into. From this approach they derive a mixing law for mixture viscosity arising from combining two liquids. For the case when the excess free energy of mixing is zero the authors derive what is often termed the ideal mixing law for two liquids[36]

$$\ln \eta = x_1 \ln \eta_1 + x_2 \ln \eta_2 \tag{2}$$

where η is the mixture viscosity, η_i is the viscosity of species i, and x_i is the mole fraction of species i. The most important result of the theory proposed by McAllister[29] and that of the work of Powell et al.[30] is that the free energy of activation for viscosity is additive on a mole fraction basis as opposed to mass or volume fractions. In 1913 it was Kendall who first pointed out that "viscosity is essentially the fractional resistance encountered by molecules of a solution in moving over one another" and so concluded that it was more logical to quantify mixtures in terms of mole rather than volume or mass fractions.[28] Kendall showed that the Arrhenius formula for mixture viscosity proposed in 1887, which was originally expressed in terms of volume fraction, had much better agreement with all of the then available data when using mole fraction.[28]

Systems in which considerable interactions are known to occur between the two components in the mixture are found to deviate from the viscosity ideal mixing law, eq 2. When plotting the natural logarithm of mixture viscosity vs mole fraction of one of the components maxima or minima are observed, as opposed to the expected linear dependence, indicating the formation of addition compounds/aggregates/hydrogen bonds/micelles or the dissociation of an associated liquid. Throughout our work we will therefore use eq 2 as a basis to quantify how far our measured viscosities deviate from an ideal mixing behavior.

In this study we use NMR to measure the microscopic properties of the [C2mim][OAc]−water mixtures. As with the viscosity it is our intention to quantify how much these microscopic parameters deviate from an ideal behavior in the mixtures. To do this we take the viscosity ideal mixing law, eq 2, and develop it in terms of the microscopic parameters. This gives us a reference frame in which to compare and contrast the effect of composition on the molecular scale.

The hydrodynamic basis for determining the rotational friction coefficient for a sphere rotating in a viscous medium was introduced by Stokes and then later used by Einstein to describe the Brownian motion of particles. The resulting Stokes−Einstein equation can be used to connect the self-diffusion coefficients of the ions and water molecules to the macroscopic viscosity through

$$D_i = \frac{kT}{6\pi f \eta R_{\mathrm{H},i}} \tag{3}$$

where D_i is the self-diffusion coefficient of component i (i = water, anion, or cation), k is the Boltzmann constant, $R_{\mathrm{H},i}$ is the hydrodynamic radius of i, η is the zero-shear rate viscosity of the medium (here the [C2mim][OAc]−water mixture at a given composition), and f is a correction term, sometimes known as the microscopic viscosity prefactor.[30,36,37] For classical Stokes−Einstein behavior the dimensionless parameter f has size unity. It can deviate from this value due to four key reasons. These are (i) the diffusing molecule is anisotropic reducing f;[38] (ii) the size of the diffusing molecule is small relative to the mixture in which it diffuses, again reducing f (in the limit that the diffusing molecule is large with respect to the solution molecules f tends to unity);[39] (iii) there are interactions, such as hydrogen bonding, with the environment in which it diffuses, making f larger; and finally (iv) the formation of aggregates that increases the effective hydrodynamic radius of the diffusing particle having the phenomenological effect of increasing f.

From eq 3 it follows that at a constant temperature $1/D_i$ is proportional to the viscosity. Therefore if the macroscopic viscosity follows an ideal mixing law, then so should the term $1/D_i$, hence

$$\ln\left(\frac{1}{D_i}\right) = x_1 \ln \frac{1}{D_{i,1}} + x_2 \ln \frac{1}{D_{i,2}} \tag{4}$$

where D_i is the self-diffusion coefficient for species i (i = anion, cation, or water) in the mixture, and $D_{i,j}$ is the self-diffusion coefficient of i in liquid j, where j = 1 corresponds to [C2mim][OAc] and 2 to water. For the case of anion and cation in pure water and vice versa, $D_{i,j}$ is taken to mean the limiting value of $D_{i,j}$ at infinite dilution. Here we take the practical approach of using the values found for 0.5% by weight of the diffusing species in 99.5% by weight solution as these values.

Mathematically eq 4 could be expressed equally in terms of D instead of $1/D$. It is more usefully written this way, though, since any deviations from this ideal mixing rule will have the same sense as those of deviations from the viscosity ideal mixing rule. A minimum will therefore reflect an increase in mobility over that predicted by the ideal mixing rules for both the viscosity and the inverse diffusion plots.

Now we turn to the NMR relaxometry measurements, T_1 and T_2. According to the classical work of Bloembergen, Purcell, and Pound (BPP),[40] the ^{1}H NMR relaxation times, in the high temperature limit, are given by[41,42]

$$\frac{1}{T_1} = \frac{1}{T_2} = 5K\tau_{rot} \quad (5)$$

where for spin 1/2 nuclei

$$K = \frac{3}{10}\left(\frac{\mu_0}{4\pi}\right)^2 \hbar^2\gamma^4 \sum_l \frac{1}{r_l^6} \quad (6)$$

and τ_{rot} is a molecular rotational correlation time, μ_0 is the permeability of free space, $\hbar$ is the reduced Planck constant, γ is the gyromagnetic ratio for protons, and r_l is the distance from a ^{1}H nucleus to its lth neighboring ^{1}H nucleus. In all our work we are in the high temperature limit and have $T_1 = T_2$, which also indicates that rotational motion dominates the NMR relaxation.[43] From now on we shall therefore only consider the one relaxation time, T_1.

In classical mechanics a spherical molecule has a rotational correlation time given by the Stokes−Einstein−Debye equation[41,44]

$$\tau_{rot} = \frac{4}{3}\pi R_H{}^3 f' \frac{\eta}{kT} \quad (7)$$

where, as before, the f' term is a correction factor similar to f in eq 3 above.[36] Combining this with eq 5 gives a relationship between T_1 and the viscosity as

$$\frac{1}{T_1} = \left(\frac{20\pi}{3} K R_H{}^3 f'\right)\frac{\eta}{kT} \quad (8)$$

Following the same reasoning as used in the construction of the ideal mixing law for the diffusion coefficients the relevant term is $1/T_1$ as it is proportional to the viscosity, so

$$\ln\left(\frac{1}{T_1}\right) = x_1 \ln\frac{1}{T_{1,1}} + x_2 \ln\frac{1}{T_{1,2}} \quad (9)$$

where $T_{1,i}$ is the T_1 value for the mixture, where 1 indicates pure water and 2 pure [C2mim][OAc]. Again any deviations from this ideal mixing rule will have the same sense as those of deviations from the viscosity and diffusion ideal mixing rules.

RESULTS

Evolution of Mixture Temperature. The evolution of mixture temperature in time from the moment when water is added to [C2mim][OAc] is presented in Figure 1. As soon as even a small amount of water is added to this IL the mixture temperature increases rapidly and significantly. The most pronounced effect was recorded for the mixture with water mole fraction of 0.7. The increase in mixture temperature can be described in terms of maximal deviation ΔT from the starting temperature T_0 via

$$\Delta T = T_{max} - T_0 \quad (10)$$

where T_{max} is the maximal temperature obtained for a given mixture composition. These results are presented in Figure 2 showing ΔT as a function of water mole fraction.

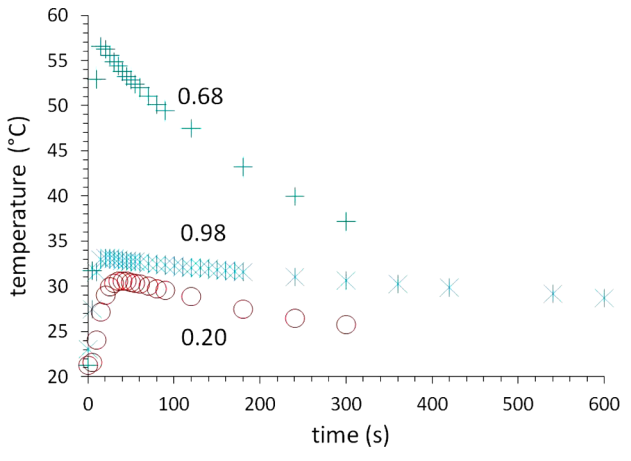

Figure 1. Examples of the evolution of mixture temperature in time; water mole fractions are shown on the graph.

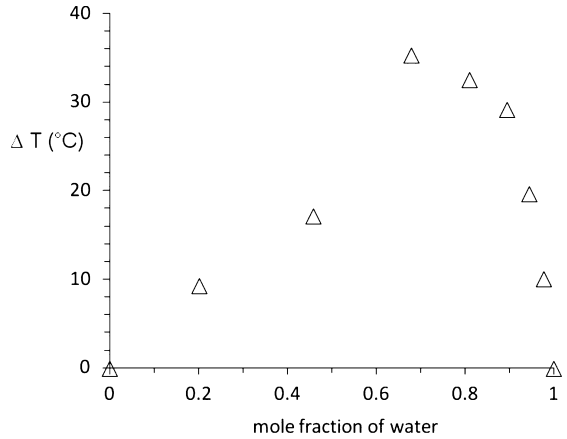

Figure 2. Maximal temperature deviation from the initial temperature as a function of mixture water mole fraction.

Density. In Figure 3 the experimental values of the [C2mim][OAc]−water mixtures densities as a function of water content are shown. The density we determined for the pure ionic liquid is within 0.5% of that reported elsewhere.[45] The solid line in Figure 3 is calculated according to a simple volume additive mixing rule

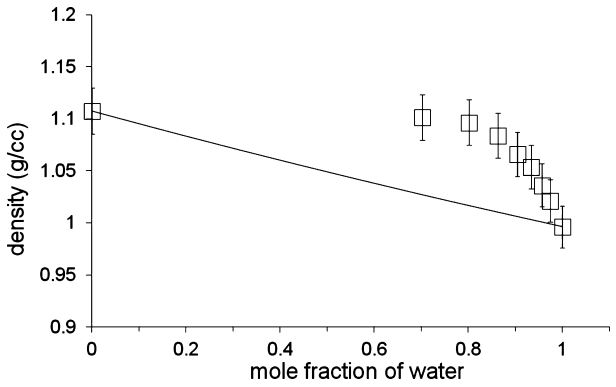

Figure 3. Density of [C2mim][OAc]−water mixtures as a function of water molar fraction, measured at 27 °C. Solid line corresponds to ρ_{calc} calculated according to additive mixing rule, eq 11.

$$\frac{1}{\rho_{calc}} = x_1\frac{1}{\rho_1} + x_2\frac{1}{\rho_2} \quad (11)$$

where ρ_{calc} is calculated mixture density, x_1 and x_2 are the molar fractions of each component, and ρ_1 and ρ_2 are the densities of the neat components. There is a clear deviation of the experimental data from the solid line.

dx.doi.org/10.1021/jp306829c | J. Phys. Chem. B 2012, 116, 12810−12818

From the density data shown in Figure 3 we calculated the excess molar volume V_{excess}, defined by[46]

$$\rho = \frac{(x_1M_1 + x_2M_2)}{(x_1V_1 + x_2V_2 + V_{excess})} \quad (12)$$

where ρ is the mixture experimental density, M_i is the molar mass of i, and V_i is the volume of 1 mol of substance i, which we calculated from the known densities of the pure components at 27 °C. The excess molar volume is shown in Figure 4.

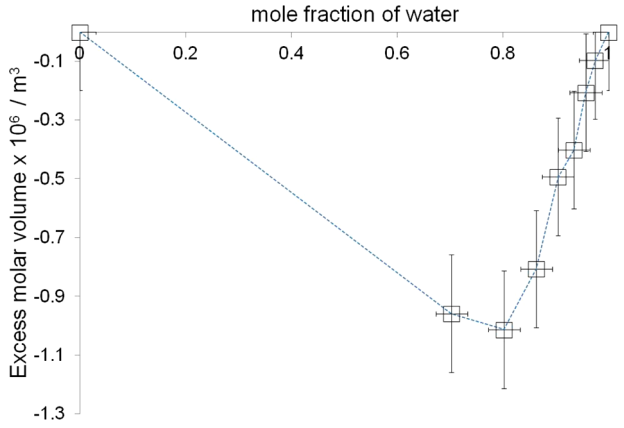

Figure 4. Excess molar volume as a function of molar fraction of water measured at 27 °C.

The excess molar volumes are negative showing that for this system the molar volumes are not additive and that the resultant mixture has a smaller volume than that of the sum of the volumes of the [C2mim][OAc] and water that have been mixed together. In other words, the mixture is made of more closely packed components with the density greater than that expected from a simple addition of molar volumes. The greatest deviation of experimental data from the calculated additive ones is around 0.80 ± 0.05. Work by Rodriguez and Brennecke looking at mixtures of ILs with water found excess molar volumes of the same order of magnitude as our data ~10^{-6} m^3 mol^{-1}, with [C2MIM] trifluoromethanesulfonate having positive excess molar volumes and [C2MIM] ethylsulfate and [C2MIM] trifluoroacetate having negative excess molar volumes.[47]

NMR Chemical Shift. For each composition of our [C2mim][OAc]−water mixtures, a proton spectrum was measured. The assigned proton resonances (1−7) for the [C2mim][OAc] molecule are shown in Figure 5. In our study proton resonance 5 was used as a reference point; we determined the chemical shift δ of the other resonances via their distances from this peak. This method follows several other ^{1}H NMR studies on imidazolium based ILs where the chemical shift of the methyl group corresponding to peak 5 has been shown to be largely independent of extrinsic variables,

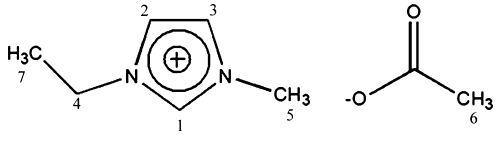

Figure 5. Chemical structure of $[C2MIM]^+$ and $[OAc]^-$ ions of 1-ethyl-3-methyl-imidazolium acetate with the proton resonances labeled (1−7).

such as IL concentration in water/1-alkyl-3-methylimidazolium bromide solutions[13] and cellobiose concentration[48] upon solvation in [C2mim][OAc].

To calculate the change in position of the peaks $\Delta\delta$ on the addition of water, we used the δ for each resonance in the sample containing 0.5% by weight water as a starting reference value, so that $\Delta\delta$ corresponds to the change in parts per million (ppm) of a peak from this starting mixture sample. In Figure 6 $\Delta\delta$ is plotted as a function of water concentration.

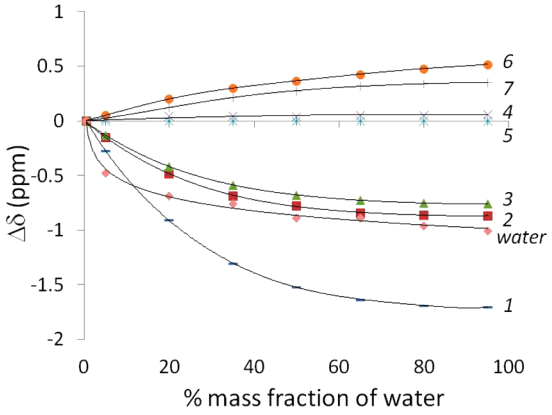

Figure 6. $\Delta\delta$ at 20 °C versus mass fraction of water for the various [C2mim][OAc] resonances (1−7), recall Figure 5, and water resonance. The lines are guides to the eye. The uncertainty in the ppm is approximately 0.05 and within the size of the data points shown.

Peak 1 shows the greatest movement in its resonance position upon the addition of water, with this being the most acidic proton (peak 1) on the imidazolium ring. All of the ring protons have negative values for their $\Delta\delta$s, corresponding to an upfield movement. This indicates that the addition of water has disrupted the dry [C2mim][OAc] hydrogen bond network. This upfield movement is consistent with recent simulation results where it was found that the water molecules compete with the anions to be positioned near to peak 1 where it then forms weaker bonds than the anion did.[49] The acetate anion forms strong hydrogen bonds with the water molecules[49] and therefore on the addition of water leaves the ring protons of the cation, causing their upfield shift. Peak 4, the CH_2 group in the alkyl chain, is not affected by the addition of water, which is in agreement with previous work.[13] Peaks 6 and 7, the two methyl groups, have a small downfield shift, with this being seen before upon the addition of cellobiose[48] and cellulose.[14] The water molecules have an upfield shift indicating that the addition of water to IL causes the water molecules to bond more strongly with the anion than they do to other water molecules. This is consistent with simulation work, which shows that with increasing [C2mim][OAc] content in these mixtures the water actually becomes more structured, revealed by higher peaks in radial distribution functions.[49] Finally, the smooth dependencies of $\Delta\delta$ for all of the peaks on the mass fraction of water indicates that this IL does not form micelles in water,[13] due to the shortness of the alkyl chain attached to the imidazolium ring. Finally, no unidentified peaks were seen in the 1H spectra indicating that if new compounds were formed they must be at very low mass fractions or short-lived to remain undetected.

Viscosity. Steady state viscosities of [C2mim][OAc]−water mixtures were measured as a function of shear rate for all compositions and temperatures studied. For each case a Newtonian plateau was measurable for at least one decade of shear rates. The mean values were calculated and used in the following to plot viscosity vs composition at various temperatures. In Figure 7 the viscosity as a function of water content is

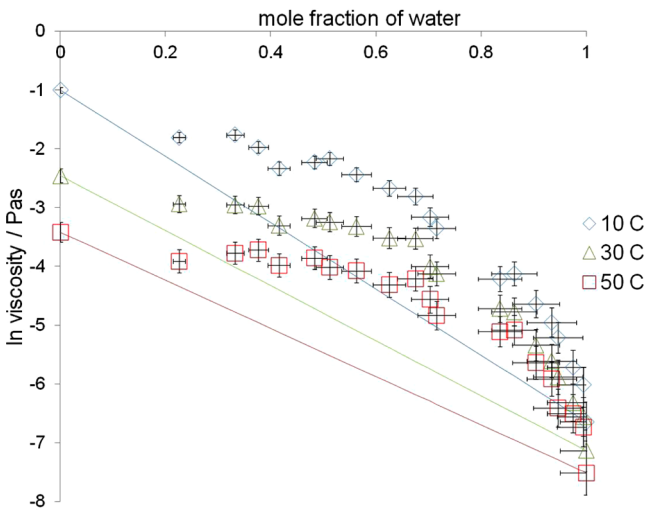

Figure 7. Mixture viscosity as a function of water molar fraction: points are experimental data at three temperatures, and solid lines are additive dependences calculated according to eq 2.

shown at three selected temperatures. The experimental viscosity data deviates from the ideal mixing law, shown as the straight lines in Figure 7, systematically having a significantly higher viscosity than predicted.

NMR Relaxometry. For all our samples and at all temperatures measured (20 to 90 °C) T_1 is equal to T_2 within 10%. This means that the data are in the high temperature limit with motion occurring on a time scale much shorter than that set by the inverse of the NMR resonance frequency of 20 MHz. It also implies that rotational,[43] as opposed to translational, motion is responsible for the NMR signal relaxation.

In Figure 8 the natural logarithm of the inverse of the longitudinal relaxation time, $\ln(1/T_1)$, is plotted against the mole fraction of water to see whether this rotational correlation time follows an ideal mixing law, recall eq 9.

In Figure 8 it can be seen that the measured $1/T_1$ values are greater than those predicted by a simple mixing rule, which means the rotational molecular correlation times responsible for the NMR relaxations are larger than expected. In [C2mim][OAc]−water mixtures the molecules are therefore finding it more difficult to reorient due to intermolecular interactions between the water and [C2mim][OAc] ions. This is consistent with our zero shear rate viscosity measurements.

NMR Diffusion. Diffusion coefficients of anion, cation, and water were measured at various mixture compositions and temperatures. We first examine diffusion data as a function of mixture composition. An example of $\ln(1/D)$ for anion, cation, and water at 40 °C is plotted against the mole fraction of water (Figure 9), similar results were obtained for other mixture temperatures. The inverse values of diffusion coefficients are higher than the corresponding ones calculated with the ideal mixing law eq 4, both for the water and ions. Figures 7

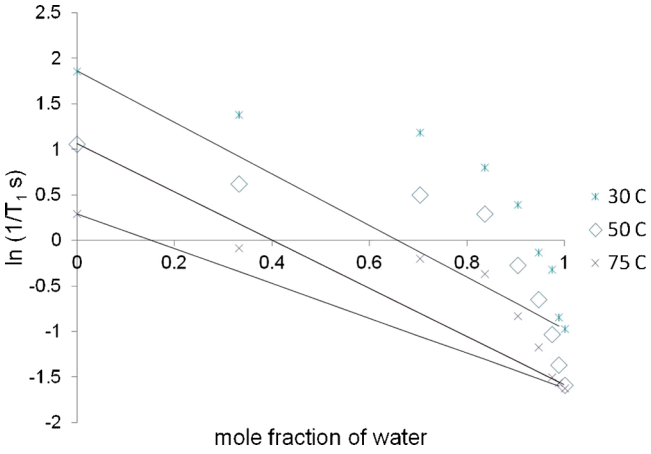

Figure 8. Natural logarithm of $1/T_1$ versus mole fraction of water. The straight lines are ideal mixing law relationships, eq 9. The uncertainty in the T_1 is approximately 5% and within the size of the data points shown.

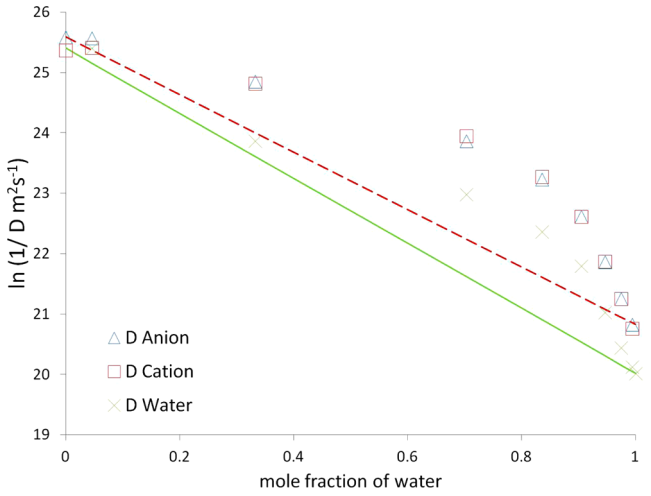

Figure 9. Inverse of the diffusion coefficients against mole fraction of water at 40 °C. The dashed line is the ideal mixing law for the ions and the solid line is that for the water molecules. The uncertainty in D is approximately 5% and within the size of the data points shown.

(viscosity), 8 (relaxometry), and 9 (diffusion) show very similar trends.

Figure 9 shows, in the first approximation and within the scale used, that diffusion coefficients of cation and anion practically coincide. However, it is known that for imidazolium-based ionic liquids (without water) the diffusion coefficient of the bulky cation is greater than that of the anion,[14] which has been explained by the anisotropic diffusion of the cation,[50] with displacements in the plane of the imidazolium ring being significantly faster than those orthogonal to it. A careful analysis shows that in the absence of water or at low water content this is what is observed in our [C2mim][OAc]−water system, the ratio D_{anion}/D_{cation} is less than 1, see Figure 10. On addition of water though this ratio "normalizes" such that the anomalous difference between the diffusion coefficients of the ions is lost. The same effect of water molecules on ILs was reported for 1-ethyl-3-methylimidazolium ethylsulfate and triflate.[3] In work by Hou et al.[51] investigating mixtures of ILs with water inside and outside Nafion membranes, similar results to ours were found for [C2mim][TfO] and [C2mim][BF_4]. For these mixtures the

dx.doi.org/10.1021/jp306829c | J. Phys. Chem. B 2012, 116, 12810−12818

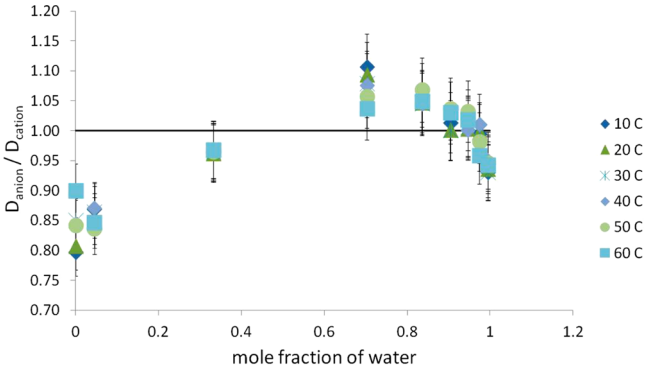

Figure 10. Ratio of the self-diffusion coefficient of the anion to the cation as a function of water mole fraction.

ratio of anion to cation diffusion coefficients increased with increasing water content, with the value for this ratio becoming greater than one at high water content. It is interesting to note that for our data at high water concentrations D_{anion}/D_{cation} starts to decrease and at water mole fraction >0.9 the diffusion of the cation seems to be quicker again than that of the anion.

In Figure 11 we have plotted the ratio of the water diffusion coefficient to that of the cation. For very small amounts of

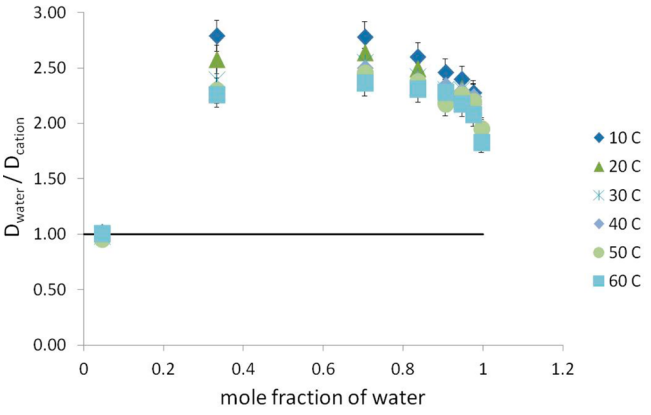

Figure 11. Ratio of the self-diffusion coefficient of the water to the cation as a function of water mole fraction.

water (~0.05 mol fraction), the water molecules have the same value for their diffusion coefficient as that for the cation. This was true for all temperatures studied and suggests some close association of the water with the cation. Indeed it has been previously found that for small water contents the interaction of the water with ionic liquid is specific and localized to the aromatic protons in the imidazolium ring.[52,53] With the increase of water content in the IL–water mixture, the water diffuses at a significantly faster rate, with a self-diffusion coefficient two to three times that of the cation, suggesting a bulk water network is established in these mixtures.

DISCUSSION

Stokes–Einstein Analysis. In Figure 12 we present plots of D for the water molecules, cations, and anions against $T/\eta(T)$ for 0.70 mol fraction of water solution, and similar results were obtained for other mixture compositions.

From Figure 12 it can be seen that all three components in the mixture (water, cation, and anion) follow the Stokes–Einstein relationship, eq 3. From the straight line fits in Figure

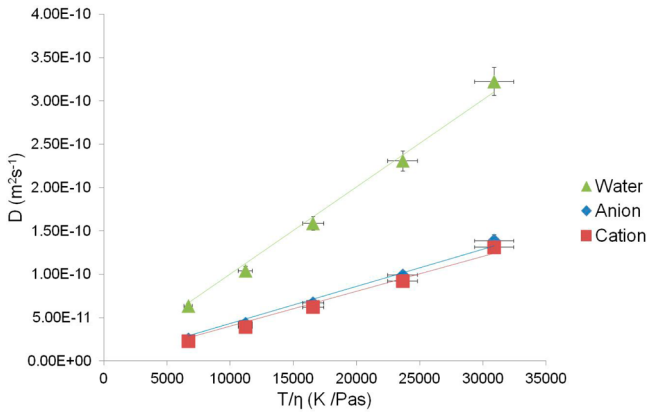

Figure 12. Correlation between D and $T/\eta(T)$ for the water molecules, cations, and anions for 0.70 mol fraction of water in the [C2mim][OAc]–water mixture. The solid straight lines are fits to eq 3.

12 and similarly for the data from the other compositions, we can determine the microscopic prefactor f in eq 3. To do this we need to first determine the hydrodynamic radii of each species. This can be done from the following equation[39] based on the work by Li and Chang[54]

$$R_H = \frac{1}{2}\left(\frac{V}{N_A}\right)^{1/3} \quad (13)$$

where V is the molar volume and N_A is the Avogadro constant. From this we calculate the hydrodynamic radius for water, cation, and anion as 1.6, 2.8, and 2.2 Å, respectively. These values agree well with other published values.[41] From the gradient of the Stokes–Einstein plots, it is now possible to calculate f, which for each species across the entire compositional range is fairly constant; for the anion, the cation, and water, f was determined at 0.71 ± 0.08, 0.58 ± 0.08, and 0.48 ± 0.09, respectively. These values are all close to but less than unity. This shows that the Stokes–Einstein relationship is correctly relating the microscopic diffusion to the macroscopic viscosity and vice versa well within 1 order of magnitude. Also, as the molecules that are diffusing within the medium are of a similar size (same order of magnitude) to those of the medium itself, then f is expected to be less than one. In the work by McLaughlin,[39] it was shown that the prefactor 6 in the Stokes–Einstein relationship should be set to 4 for molecules diffusing within a medium of like sized molecules. This is equivalent in our analysis to setting $f = 4/6$, which is remarkably close to the anion result (0.71 ± 0.08) obtained above. Interestingly the anion is therefore not diffusing slower[11] than expected. Our work also supports simulation results, which find that it is the cation that is "anomalous" in that it diffuses faster than expected,[50] i.e. here it has an $f < 4/6$. Finally, our analysis reveals that it is the water molecules that experience the lowest microviscosity.

NMR Relaxometry–Viscosity. In Figure 13, $1/T_1$ is plotted against the viscosity divided by temperature to look for the direct proportionality predicted by eq 8.

The linear dependence displayed in Figure 13 was found for the data from all our sample compositions. This result and the Stokes–Einstein plots in Figure 12 together reveal that microscopically the local microviscosity for both rotational and translational motion must be proportional to the

dx.doi.org/10.1021/jp306829c | J. Phys. Chem. B 2012, 116, 12810–12818

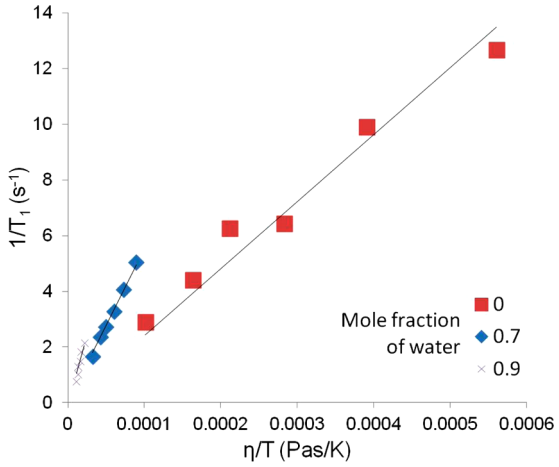

Figure 13. $1/T_1$ versus viscosity over temperature. The solid lines are fits to eq 8.

macroscopic viscosity and furthermore this constant of proportionality is independent of temperature.

Ideal Mixing Law. All our data deviate from their ideal mixing laws. We will now compare all our measurements by calculating for each one the percentage difference between the measured value and the corresponding one given by the mixing rule, as discussed in the Background section:

$$\%\text{difference} = \frac{\text{measured} - \text{ideal mixing result}}{\text{ideal mixing result}} \times 100 \tag{14}$$

In Figure 14 all our data are combined showing how much each parameter deviates from its ideal mixing rule. We did not plot the cation diffusion data because it is close to the anion data, recall Figure 10.

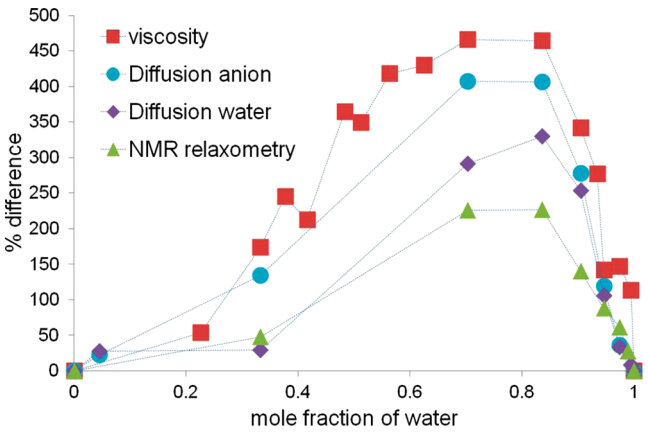

Figure 14. Percent difference between measured parameters and the corresponding simple ideal mixing predictions for viscosity, anion inverse diffusion, water inverse diffusion and inverse spin−lattice relaxation. The dashed lines are guides to the eye.

In Figure 14 it can be seen that the maximum deviations from the ideal mixing rules occur for all our data at 0.75 ± 0.05 mol fraction of water, which is also where the minimum in excess molar volume occurred, recall Figure 4, and where the greatest change in mixture temperature upon the addition of water to IL was found, Figure 2. The position of these peaks occurs at a water concentration that corresponds to three water molecules per [C2mim][OAc] molecule.

CONCLUSIONS

We have investigated mixtures of [C2mim][OAc] and water across the entire composition range, from pure [C2mim][OAc] to pure water, using density, viscosity, and NMR spectroscopy, relaxometry, and diffusion measurements.

On preparation of the samples, it was found that adding water to [C2mim][OAc] caused the mixtures to significantly increase in temperature. A maximum increase of 35 ± 2 °C was found to occur for the mixture consisting of a water mole fraction 0.68 ± 0.07.

The excess molar volumes were calculated from the density measurements. These were found to be negative and of approximately cm^3/mol with a minimum occurring at a mole fraction of water 0.80 ± 0.08.

The change in ^{1}H chemical shift positions $\Delta\delta$ revealed that the resonances 1−3 belonging to the imidazolium ring protons had the strongest dependencies on water composition, with them moving upfield on the addition of water. This is consistent with the explanation that the anion preferentially forms hydrogen bonds with the water molecules, separating from the cations in order to do so. The dependence of $\Delta\delta$ for each resonance on water composition does not indicate the formation of micelles presumably because longer attached alkyl chains are needed for micelle formation to occur.

The Newtonian viscosities for all our samples were recorded. The viscosities deviated from a simple ideal mixing law being significantly higher than expected from this rule. A peak difference occurred at the composition of 0.70 ± 0.07 mol fraction of water.

Low field (20 MHz) proton spin−lattice (T_1) and spin−spin relaxation (T_2) times were measured. It was found that for all our samples and all temperatures measured $T_1 = T_2$ within experimental uncertainty. This suggests that rotation motion is the dominant physical mechanism for the NMR measured relaxation. These parameters are therefore measuring the average local rotational microviscosity. A simple ideal mixing law was developed for T_1, see eq 9. The data deviated from this mixing rule with the samples showed a higher local microviscosity, or higher ($1/T_1$), than expected. Again a peak was found to occur for the deviation from the mixing rule at 0.77 ± 0.07 mol fraction of water.

High field NMR (400 MHz) was used to measure the self-diffusion coefficients for each component (anion/cation/water) in our mixtures. The cation was found to have a higher diffusion coefficient than the anion in the pure IL, with the addition of water causing them to become equal, recall Figure 10. For very low concentrations of water (0.5% by weight), the water molecules had the same value for their self-diffusion coefficient as that of the cation, suggesting that their movements in the mixture are correlated. For the rest of the samples the water molecules had a diffusion coefficient two to three times that of the cation. Again a simple ideal mixing rule for the diffusion coefficients was developed, recall eq 4. The data likewise deviated from this mixing rule, with the translational motion being found to be slower than expected, with a peak difference for each component occurring at 0.77 ± 0.07.

The diffusion data was compared with the macroscopic viscosity data and found to follow the Stokes−Einstein relationship. We interpreted the slopes of the graphs diffusion vs $T/\eta(T)$ in terms of a local microviscosity prefactor f. The

dx.doi.org/10.1021/jp306829c | J. Phys. Chem. B 2012, 116, 12810−12818

anions follow the Stokes−Einstein prediction most closely in that they have f nearest to unity. The cations and water molecules have lower values for f indicating that they experience a smaller local microviscosity than that compared with the value set by the Newtonian macroscopic viscosity.

AUTHOR INFORMATION

Corresponding Author

*E-mail: m.e.ries@leeds.ac.uk.

Notes

The authors declare no competing financial interest.

ACKNOWLEDGMENTS

M.E.R. is grateful to the Royal Society International Outgoing Short Visit Grant 2008/R3 and EPSRC seed money EP/I500286/1. A.R. is funded by the Malaysian Government. C.A.H. is funded by the Nuffield Institute. The research of K.A.L. has received funding from the European Union Seventh Framework Programme (FP7/2007-2013) under grant agreement No. 214653, project "SurFunCell". C.R. is funded by French National Research Agency (ANR), project "Nanocel" ANR-09-HABISOL-010.

REFERENCES

(1) Ficke, L. E.; Brennecke, J. F. *J. Phys. Chem. B* **2010**, *114*, 10496.
(2) Wang, H.; Gurau, G.; Rogers, R. D. *Chem. Soc. Rev.* **2012**, *41*, 1519.
(3) Menjoge, A.; Dixon, J.; Brennecke, J. F.; Maginn, E. J.; Vasenkov, S. *J. Phys. Chem. B* **2009**, *113*, 6353.
(4) Seddon, K. R.; Stark, A.; Torres, M. J. *Pure Appl. Chem.* **2000**, *72*, 2275.
(5) Bowron, D. T.; D'Agostino, C.; Gladden, L. F.; Hardacre, C.; Holbrey, J. D.; Lagunas, M. C.; McGregor, J.; Mantle, M. D.; Mullan, C. L.; Youngs, T. G. A. *J. Phys. Chem. B* **2010**, *114*, 7760.
(6) Chen, T.; Chidambaram, M.; Lin, Z.; Smit, B.; Bell, A. T. *J. Phys. Chem. B* **2010**, *114*, 5790.
(7) Feng, S.; Voth, G. A. *Fluid Phase Equilib.* **2010**, *294*, 148.
(8) Karimi-Varzaneh, H. A.; Mueller-Plathe, F.; Balasubramanian, S.; Carbone, P. *Phys. Chem. Chem. Phys.* **2010**, *12*, 4714.
(9) Spohr, H. V.; Patey, G. N. *J. Chem. Phys.* **2010**, 132.
(10) Chung, S. H.; Lopato, R.; Greenbaum, S. G.; Shirota, H.; Castner, E. W., Jr.; Wishart, J. F. *J. Phys. Chem. B* **2007**, *111*, 4885.
(11) Remsing, R. C.; Hernandez, G.; Swatloski, R. P.; Massefski, W. W.; Rogers, R. D.; Moyna, G. *J. Phys. Chem. B* **2008**, *112*, 11071.
(12) Xu, Y.; Gao, Y.; Zhang, L.; Yao, J.; Wang, C.; Li, H. *Sci. Chin.-Chem.* **2010**, *53*, 1561.
(13) Zhao, Y.; Gao, S. J.; Wang, J. J.; Tang, J. M. *J. Phys. Chem. B* **2008**, *112*, 2031.
(14) Lovell, C. S.; Walker, A.; Damion, R. A.; Radhi, A.; Tanner, S. F.; Budtova, T.; Ries, M. E. *Biomacromolecules* **2010**, *11*, 2927.
(15) Sescousse, R.; Le, K. A.; Ries, M. E.; Budtova, T. *J. Phys. Chem. B* **2010**, *114*, 7222.
(16) Le, K. A.; Sescousse, R.; Budtova, T. *Cellulose* **2012**, *19*, 45.
(17) Fendt, S.; Padmanabhan, S.; Blanch, H. W.; Prausnitz, J. M. *J. Chem. Eng. Data* **2011**, *56*, 31.
(18) Cornellas, A.; Perez, L.; Comelles, F.; Ribosa, I.; Manresa, A.; Garcia, M. T. *J. Colloid Interface Sci.* **2011**, *355*, 164.
(19) Jungnickel, C.; Luczak, J.; Ranke, J.; Fernandez, J. F.; Muller, A.; Thoming, J. *Colloids Surf. A-Physicochem. Eng. Aspects* **2008**, *316*, 278.
(20) Luczak, J.; Hupka, J.; Thoming, J.; Jungnickel, C. *Colloids Surf. A-Physicochem. Eng. Aspects* **2008**, *329*, 125.
(21) Luczak, J.; Jungnickel, C.; Joskowska, M.; Thoming, J.; Hupka, J. *J. Colloid Interface Sci.* **2009**, *336*, 111.
(22) Wang, H. Y.; Wang, J. J.; Zhang, S. B.; Xuan, X. P. *J. Phys. Chem. B* **2008**, *112*, 16682.
(23) Wu, D.; Wu, B.; Zhang, Y. M.; Wang, H. P. *J. Chem. Eng. Data* **2010**, *55*, 621.
(24) Wu, B.; Liu, Y.; Zhang, Y. M.; Wang, H. P. *Chem.—Eur. J.* **2009**, *15*, 6889.
(25) Zhang, Q. G.; Wang, N. N.; Yu, Z. W. *J. Phys. Chem. B* **2010**, *114*, 4747.
(26) Shekaari, H.; Armanfar, E. *J. Chem. Eng. Data* **2010**, *55*, 765.
(27) Umebayashi, Y.; Jiang, J. C.; Shan, Y. L.; Lin, K. H.; Fujii, K.; Seki, S.; Ishiguro, S. I.; Lin, S. H.; Chang, H. C. *J. Chem. Phys.* **2009**, *130*, 6.
(28) Kendall, J.; Monroe, K. P. *J. Am. Chem. Soc.* **1917**, *39*, 1787.
(29) McAllister, R. A. *AIChE J.* **1960**, *6*, 427.
(30) Powell, R. E.; Roseveare, W. E.; Eyring, H. *Ind. Eng. Chem.* **1941**, *33*, 430.
(31) Annat, G.; MacFarlane, D. R.; Forsyth, M. *J. Phys. Chem. B* **2007**, *111*, 9018.
(32) Carr, H. Y.; Purcell, E. M. *Phys. Rev.* **1954**, *94*, 630.
(33) Meiboom, S.; Gill, D. *Rev. Sci. Instrum.* **1958**, *29*, 688.
(34) Holz, M.; Heil, S. R.; Sacco, A. *Phys. Chem. Chem. Phys.* **2000**, *2*, 4740.
(35) Cotts, R. M.; Hoch, M. J. R.; Sun, T.; Markett, J. T. *J. Magn. Reson.* **1989**, *83*, 252.
(36) Gisser, D. J.; Ediger, M. D. *J. Phys. Chem.* **1993**, *97*, 10818.
(37) Antony, J. H.; Dolle, A.; Mertens, D.; Wasserscheid, P.; Carper, W. R.; Wahlbeck, P. G. *J. Phys. Chem. A* **2005**, *109*, 6676.
(38) Boere, R. T.; Kidd, R. G. Rotational Correlation Times in Nuclear Magnetic Relaxation. In *Annual Reports on NMR Spectroscopy*; Webb, G. A., Ed.; Academic Press: New York, 1982; Vol. *13*, pp 319.
(39) McLaughlin, E. *Trans. Faraday Soc.* **1959**, *55*, 28.
(40) Bloembergen, N.; Purcell, E. M.; Pound, R. V. *Phys. Rev.* **1948**, *73*, 679.
(41) Carper, W. R.; Mains, G. J.; Piersma, B. J.; Mansfield, S. L.; Larive, C. K. *J. Phys. Chem.* **1996**, *100*, 4724.
(42) Hayamizu, K.; Tsuzuki, S.; Seki, S.; Umebayashi, Y. *J. Chem. Phys.* **2011**, 135.
(43) Corsaro, C.; Spooren, J.; Branca, C.; Leone, N.; Broccio, M.; Kim, C.; Chen, S. H.; Stanley, H. E.; Mallamace, F. *J. Phys. Chem. B* **2008**, *112*, 10449.
(44) See ref 38.
(45) Shiflett, M. B.; Yokozeki, A. *J. Chem. Eng. Data* **2009**, *54*, 108.
(46) Pal, A.; Gaba, R. *Chin. J. Chem.* **2007**, *25*, 1781.
(47) Rodriguez, H.; Brennecke, J. F. *J. Chem. Eng. Data* **2006**, *51*, 2145.
(48) Zhang, J. M.; Zhang, H.; Wu, J.; Zhang, J.; He, J. S.; Xiang, J. F. *Phys. Chem. Chem. Phys.* **2010**, *12*, 1941.
(49) Brehm, M.; Weber, H.; Pensado, A. S.; Stark, A.; Kirchner, B. *Phys. Chem. Chem. Phys.* **2012**, *14*, 5030.
(50) Urahata, S. M.; Ribeiro, M. C. C. *J. Chem. Phys.* **2005**, *122*, 9.
(51) Hou, J. B.; Zhang, Z. Y.; Madsen, L. A. *J. Phys. Chem. B* **2011**, *115*, 4576.
(52) Mele, A.; Tran, C. D.; Lacerda, S. H. D. *Angew. Chem., Int. Ed.* **2003**, *42*, 4364.
(53) Moreno, M.; Castiglione, F.; Mele, A.; Pasqui, C.; Raos, G. *J. Phys. Chem. B* **2008**, *112*, 7826.
(54) Li, J. C. M.; Chang, P. *J. Chem. Phys.* **1955**, *23*, 518.